A Comparison of Discrete Fracture Models for Single Phase Flow in Porous Media by COMSOL Multiphysics® Software

C. A. Romano-Perez[*1] and M. A. Diaz-Viera[2]
[1]Facultad de Ingeniería, Universidad Nacional Autónoma de México, [2]Instituto Mexicano del Petróleo
*Corresponding author: Av. Universidad # 3000, Coyoacán, Ciudad Universitaria, 04510, México D. F., carlos_alberto@comunidad.unam.mx

Abstract: A comparison of discrete fracture and explicit fracture models for single-phase flow in fractured porous media using COMSOL Multiphysics is presented to understand the contribution of each individual fracture to fluid flow, and the exchange between fracture and surrounding medium at a scale such that the fractures could be modeled explicitly. The derived flow models are based on the fluid pressure and considering the Darcy's law for fluid velocity in the porous media and the fractures, it is assumed that the fractures are filled with a porous material. The models are numerically validated in an injection-production case study in two dimensions.

Keywords: Flow, porous media, fracture, discrete fracture.

1. Introduction

A meaningful percent of hydrocarbon reserves in the world are trapped in naturally fractured reservoirs, which have usually a lower recovery factor in comparison with unfractured reservoirs. The remaining oil volume in this kind of reservoirs represents a great opportunity to increase the recovery factor applying enhanced recovery process. To implement these optimal recovery methods is necessary to develop more accurate models that describe the impact in the flow and transport of fluids in presence of complex fracture networks. Therefore fracture flow models that allow us to understand the behavior of the flow of fluids in these kind of reservoirs, considering the special characteristics of storage and matrix-fracture exchange of fluids are required.

Discrete fracture model approach basically consists in representing fractures as $(n-1)$ dimensional objects in an n-dimensional domain, i.e., in 2D fractures could be represented by line segments and in 3D by polygons, respectively.

Two discrete fracture models are here presented. In the first one fractures are represented as internal boundaries partitioning a domain into subdomains. This method will be named as a *domain decomposition* approach. While in the second one fractures are represented by embedded internal boundaries. Both models take into account interactions between the fractures and the surrounding porous medium. The numerical implementation is carried out applying the PDE coefficient mode and weak PDE form to describe flow along the interior boundaries. A third model, a explicit fracture one, considering fractures as a porous medium subdomain with different petrophysical (porosity and permeability) properties is implemented as a reference case for comparison proposes.

2. Conceptual Model

The following hypotheses are considered:
- There are two phases: fluid and solid.
- The rock and the fluid are slightly compressible.
- The fluid viscosity is constant.
- The porous medium is considered homogeneous and isotropic.
- The porous medium contains fractures.
- The fractures are considered to be another porous medium with different porosity and permeability properties.
- The porous medium and the fractures are fully saturated.
- The flow in the porous media and fractures follows the Darcy's law.
- It is considered to be an isothermal system.

3. Mathematical Models

All the models are derived applying the axiomatic formulation for continuum systems (Allen et al. 1988) and considering the assumptions established in the conceptual model.

3.1 Single Phase Flow Model in a Porous Medium

A single phase flow model in a homogeneous and isotropic porous medium for a slightly compressible fluid is obtained by a fluid mass balance equation in terms of the pressure as follows (Chen et al. 2006):

$$\phi c_t \frac{\partial p}{\partial t} - \nabla \cdot \left(\frac{\underline{\underline{k}}}{\mu} \cdot \nabla p \right) = q \qquad (1)$$

Here, the velocity $\underline{u}$ is given by the Darcy's law

$$\underline{u} = -\frac{\underline{\underline{k}}}{\mu} \cdot \nabla p \qquad (2)$$

And ϕ is the porosity, c_t is the total compressibility, $\underline{\underline{k}}$ is the absolute permeability tensor, μ is the viscosity, p is the pressure and q is the source term.
The total compressibility can be expressed as

$$c_t = c_r + c_f \qquad (3)$$

where c_f is the fluid compressibility and c_r is the rock compressibility.

3.2 Explicit Fracture Flow Model

In this model two different porous media, represented in separated subdomains, are considered. One of them is a *fracture* (f) and the other one is a porous *matrix* (m), as is schematically presented in the Figure 1. Consequently, the model consist on two coupled flow equations with the same form of equation(1) for each subdomain in terms of the pressures p^f and p^m, respectively. The internal boundary conditions are flow continuity.

3.3 Domain Decomposition Approach

This discrete fracture model is based on a domain decomposition approach and its derivation is given in (Martin et al. 2005).

The model consist in two separated subdomains divided by an internal boundary. Each subdomain represents a porous media (m_1 and m_2) and the internal boundary represent a fracture (f), as can be seen in the Figure 2.

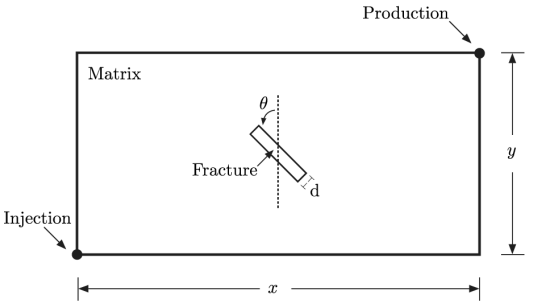

Figure 1. Schematic representation of the geometrical configuration of the explicit fracture model.

Consequently, the model is made of two flow equations, as equation (1), for each subdomain in terms of the pressures p^1 and p^2, respectively. But there is an additional flow equation for the fracture, as follows:

$$d\phi^f c_t^f \frac{\partial P^f}{\partial t} + \nabla_\tau \cdot \left(\underline{U}^f \right) = \left(\underline{u}^1 - \underline{u}^2 \right) \cdot \underline{n} + Q_{fr} \qquad (4)$$

where $\underline{n}$ is the unit vector normal to the fracture plane which can be oriented in two equivalent ways; $\underline{u}^1$ is the seepage velocity in the matrix on the side of n and $\underline{u}^2$ is the seepage velocity on the opposite side.

Here, $\underline{U}^f$ is the velocity in the direction tangential to the fracture

$$\underline{U}^f = -\frac{d}{\mu} \underline{\underline{k}}_\tau^f \cdot \nabla_\tau P^f \qquad (5)$$

where d is the fracture thickness, c_t^f is the total compressibility, μ is the viscosity, $\underline{\underline{k}}_\tau^f$ is the permeability tensor, P^f is the averaged pressure, is the outward and ∇_τ denote the tangential gradient operator.

Average pressure in the fracture

$$P^f = \frac{1}{d} \int_{-d/2}^{d/2} p^f d\underline{n} \qquad (6)$$

Fracture source term

$$Q^f = \int_{-d/2}^{d/2} q^f d\underline{n} \qquad (7)$$

The flow in the fracture is governed by a conservation equation with a source term representing flow into the fracture from the

matrix and a Darcy law relating the tangential component of the gradient of the averaged pressure to the tangential component of the averaged Darcy velocity.

The model is derived through a process of averaging across the fracture, is obtained a flow equation along the fracture that is coupled with flow equations in the porous media through Robin type conditions imposed at the interface.

The external boundary conditions are no flow while the internal boundary conditions are:

$$-\frac{1}{2}\left(\underline{u}^{1}\cdot\underline{n}_{1}\right)\Big|_{\Sigma_1}+\alpha^{f}\,p^{1}\Big|_{\Sigma_1} = -\frac{1}{2}\left(\underline{u}^{2}\cdot\underline{n}_{2}\right)\Big|_{\Sigma_2}+\alpha^{f}P^{f} \tag{8}$$

$$-\frac{1}{2}\left(\underline{u}^{2}\cdot\underline{n}_{2}\right)\Big|_{\Sigma_2}+\alpha^{f}\,p^{2}\Big|_{\Sigma_2} = -\frac{1}{2}\left(\underline{u}^{1}\cdot\underline{n}_{1}\right)\Big|_{\Sigma_1}+\alpha^{f}P^{f} \tag{9}$$

where $\alpha^{f}=\dfrac{2\underline{\underline{k}}_{n}^{fr}}{\mu d}$

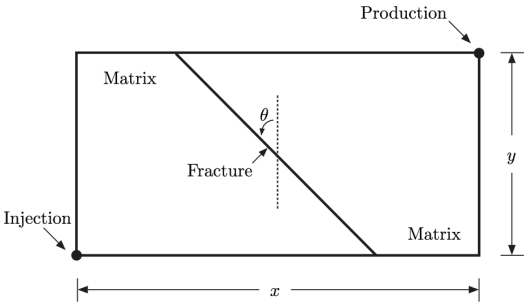

Figure 2. Schematic representation of the geometrical configuration of the domain decomposition approach.

3.4 Embedded Fracture Approach

This embedded fracture approach is very similar to the domain decomposition approach. The main differences are the following:
- There is a single porous matrix domain in which the fracture is embedded, as can be seen in the Figure 3.
- The fracture is represented as an internal boundary
- The internal boundary conditions are

$$p^{2}\Big|_{\Sigma_2}-p^{1}\Big|_{\Sigma_1} = \frac{\mu d}{2\underline{\underline{k}}_{n}^{f}}\left(\left(\underline{u}^{2}\cdot\underline{n}_{2}\right)\Big|_{\Sigma_2}-\left(\underline{u}^{1}\cdot\underline{n}_{1}\right)\Big|_{\Sigma_1}\right) \tag{10}$$

$$p^{2}\Big|_{\Sigma_2}+p^{1}\Big|_{\Sigma_1}=2P^{f} \tag{11}$$

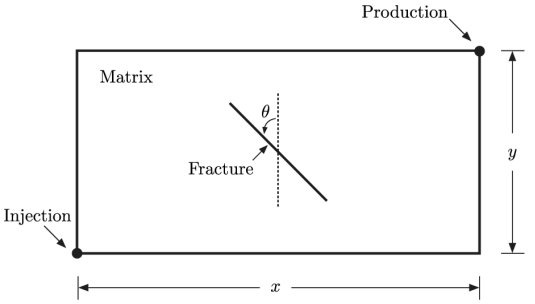

Figure 3. Schematic representation of the geometrical configuration of the embedded fracture approach.

3.5 Initial and Boundary Conditions

Initial conditions:

$$p\left(t_{0}\right)=p_{0} \tag{12}$$

Boundary conditions:
The boundary conditions specified below are considering a particular domain, which is a 2D rectangular area where fluid is injected at one corner and produced at the opposite corner.
a.) Inlet conditions (constant injection rate) at the injection corner

$$q=q_{i} \tag{13}$$

b.) Outlet conditions (constant pressure) at the production corner

$$p=p_{p} \tag{14}$$

where p_p is a production pressure.

c.) No-flow conditions at all external boundaries.

$$\underline{u}\cdot\underline{n}=0 \tag{15}$$

4. Numerical and Computational Models

In this case the resulting problem is a linear system of partial differential equations with initial and boundary conditions. For the numerical solution we apply the following methods:
- A backward finite difference discretization of second order for the temporal derivatives was used resulting a full implicit scheme in time.

- A standard finite element discretization with quadratic Lagrange polynomials.
- An unstructured mesh with triangular elements in 2D.
- A variant of the LU direct method for non-symmetric and sparse matrices, implemented in the UMFPACK library, for the solution of the resulting algebraic system of equations.

The implementation of the computational model was performed using the COMSOL Multiphysics software by the PDE modes, coefficient and weak form, for the time-dependent analysis.

5. Case Study Description

The case study is divided in two sub-cases with the aim to consider two types of fractures. In the first sub-case the fractures have a permeability higher than the matrix, and in the second the permeability is lower than that in the matrix. The data used for the case study has been taken from (Hoteit and Firoozabadi 2008, Chen et al. 2006), see Table 1.

We consider a rock matrix with a single fracture at different orientations and compare the results from the discrete-fracture models with an explicit fracture model for validation. Figure 1 represents the geometrical configuration. We inject fluid at the bottom left corner and produce from the top right corner.

6. Numerical Simulations

Simulations are carried out for four different orientations of the fractures. The number of mesh elements for each configuration of the fracture is presented in Table 2. There are more mesh elements for the explicit fracture model because of a geometry with a high aspect ratio which requires a dense mesh consisting of great number of tiny elements.

6.1 Case A: Fracture more permeable than the porous medium.

Figure 4 displays pressure profiles at 120 seconds of fluid injection-production considering a single vertical fracture ($\theta = 0°$). The main flow direction is normal to the fracture plane. We see that the behavior of domain decomposition model matches to the explicit fracture model.

Table 1: Data for all flow models.

Property (Notation)	Value [Unit]
Initial pressure ($p0$)	300 [psi]
Fluid viscosity (μ)	1.06 [cP]
Matrix permeability (k)	10 [md]
High fracture permeability (k^{fr})	10^4 [md]
Low fracture permeability (k^{fr})	10^{-7} [md]
Fluid compressibility (c_f)	0.00001 [psi^{-1}]
Rock compressibility (c_r)	0.000004 [psi^{-1}]
Fracture compressibility (c_{fr})	0.000004 [psi^{-1}]
Matrix porosity (ϕ)	0.2 [$m^3\ m^{-3}$]
Fracture porosity (ϕ_{fr})	0.2 [$m^3\ m^{-3}$]
Injection rate (q_i)	0.115 [PV day^{-1}]
Production pressure (p_p)	300 [psi]
Formation thickness (H)	1 [m]
Fracture thickness (d)	3.048 [mm]
Length in the x direction	6.096 [m]
Length in the y direction	3.048 [m]

Table 2: Number of triangular elements for the discrete fracture and explicit fracture models; Single fracture configuration.

θ	Explicit fracture	Discrete fracture	
		Domain decomposition	Embedded fracture
0°	8,300	346	336
45°	8,048	342	338
90°	8,048	332	332
-45°	8,160	338	338

The embedded fracture model does not match to the explicit fracture model.

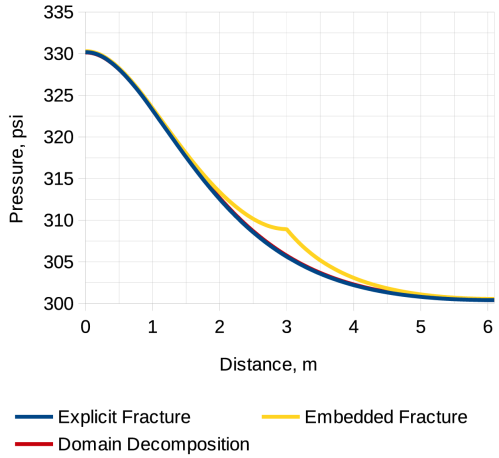

Figure 4. Pressure profile at 120 seconds of fluid injection-production considering a single vertical fracture ($\theta = 0°$).

In the Figure 5 pressure profiles for fluid injection-production at 120 seconds are shown. A single horizontal fracture ($\theta = 90°$) is considered. The main flow direction is parallel to the fracture plane. It can be seen that the behavior of the embedded fracture model gets closer to the explicit fracture and the domain decomposition models.

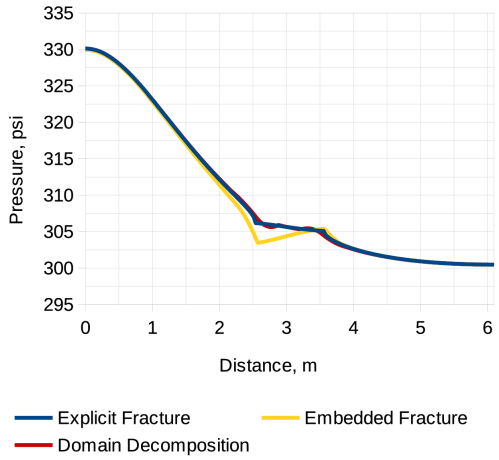

Figure 5. Pressure profile at 120 seconds of fluid injection-production considering a single horizontal fracture ($\theta = 90°$).

Figure 6 represents pressure profiles at 120 seconds of fluid injection-production considering a single tilted fracture ($\theta = 45°$). The main flow direction is normal to the fracture plane. Only the domain decomposition model matches to the explicit fracture model.

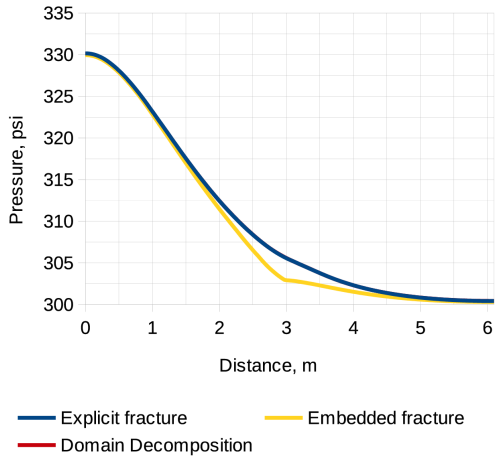

Figure 6. Pressure profile at 120 seconds of fluid injection-production considering a single tilted fracture ($\theta = 45°$).

It can be seen in the Figure 7 that for 120 seconds of fluid injection-production considering a single titled fracture ($\theta = -45°$) the domain decomposition model is very close to the explicit fracture model as long as the embedded fracture model has a similar behavior to the explicit fracture model.

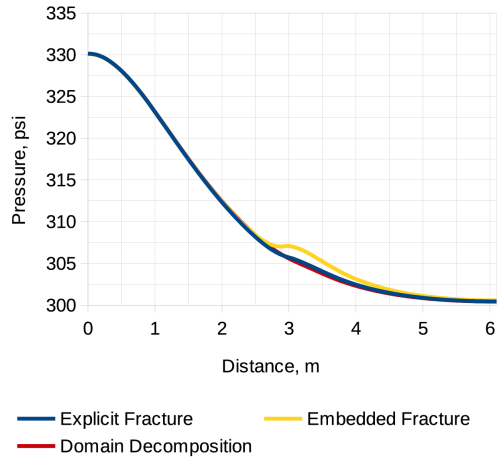

Figure 7. Pressure profile at 120 seconds of fluid injection-production considering a single tilted fracture ($\theta = -45°$).

In case A, for the four different fracture orientations, we observe the expected behavior of the pressure: pressure is a continuous function through the porous media and the fracture.

6.2 Case B: Fracture less permeable than the porous medium.

Figure 8 displays pressure profiles at 120 seconds of fluid injection-production considering a single vertical fracture ($\theta = 0°$). The main flow direction is normal to the fracture plane. We see that the behavior of domain decomposition model matches to the explicit fracture model. The embedded fracture model has a similar behavior to the explicit fracture model.

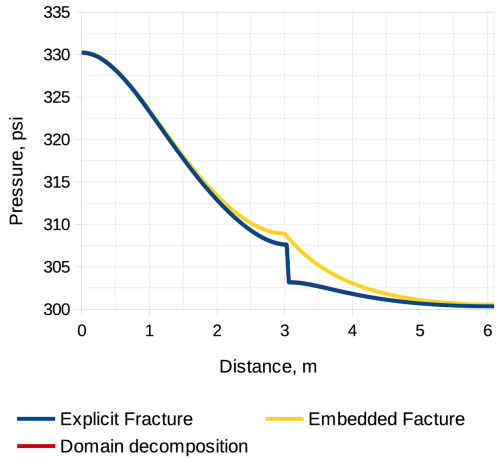

Figure 8. Pressure profile at 120 seconds of fluid injection-production considering a single vertical fracture ($\theta = 0°$).

In the Figure 9 pressure profiles for fluid injection-production at 120 seconds is shown. A single horizontal fracture ($\theta = 90°$) is considered. The main flow direction is parallel to the fracture plane. It can be seen that neither the behavior of the domain decomposition model nor embedded fracture model do not match to the explicit fracture model.

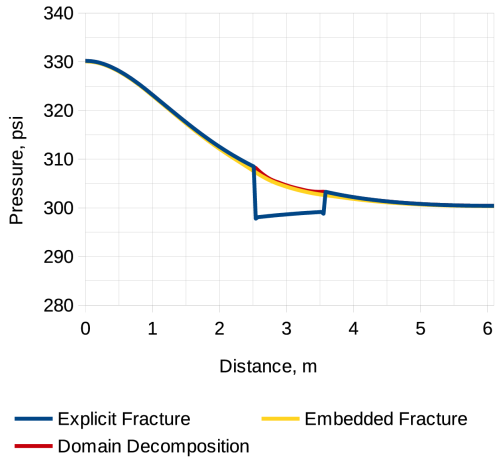

Figure 9. Pressure profile at 120 seconds of fluid injection-production considering a single horizontal fracture ($\theta = 90°$).

Figure 10 represents pressure profiles at 120 seconds of fluid injection-production considering a single tilted fracture ($\theta = 45°$). The main flow direction is normal to the fracture plane. The domain decomposition model behavior matches to the explicit fracture model.

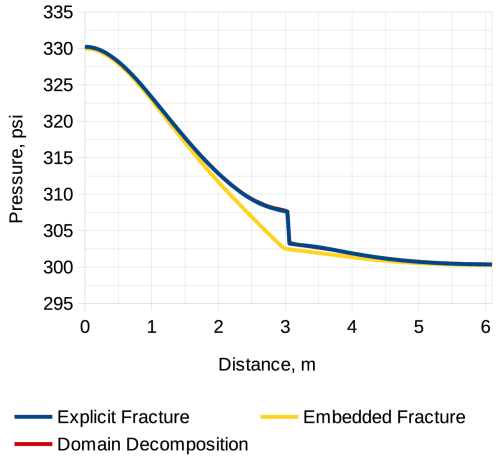

Figure 10. Pressure profile at 120 seconds of fluid injection-production considering a single tilted fracture ($\theta = 45°$).

It can be seen in the Figure 11 that for 120 seconds of fluid injection-production considering a single titled fracture ($\theta = -45°$) again, the domain decomposition model behavior matches to the explicit fracture model.

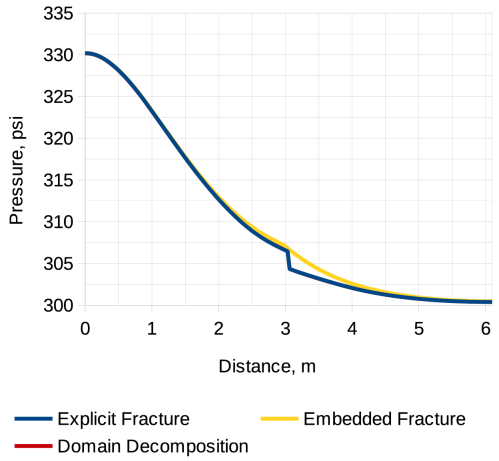

Figure 11. Pressure profile at 120 seconds of fluid injection-production considering a single tilted fracture ($\theta = -45°$).

The embedded fracture model was not satisfactory for Case B: Fracture less permeable than the porous medium.

For the four different fracture orientations, we observe the expected behavior of the pressure in the domain decomposition model: the pressure is not continuous across the fracture-interface.

8. Conclusions

Discrete fracture models compared to explicit fracture model have the advantage that for the same order of accuracy the number of elements in the mesh are reduced significantly and, consequently, they have a better computational performance since it involves fewer degrees of freedom (unknowns).

The discrete fracture model using the domain decomposition approach can adequately represent the flow in both cases when the fracture permeability is higher or lower with respect to matrix permeability. In particular, its approximation is better when the main flow direction is normal to the fracture plane. However, this approach is much more complicated and difficult to implement and is not a practical alternative for fracture flow modeling in porous media.

The discrete fracture model using the embedded fracture approach is much more simple and flexible to implement in comparison with the domain decomposition approach. This approach can represent properly the flow if the fracture is more permeable than the porous medium but not in the opposite case. And its accuracy is better when the main flow direction is parallel to the fracture plane.

Since in oil recovery process modeling, the case where the fracture has higher permeability than the surrounding porous medium usually is more significant than the case where the fracture has lower permeability, the embedded fracture approach could represent a viable alternative to model flow through a discrete fracture network in porous media.

9. References

1. Allen, M.B., Herrera, I. and Pinder, G.F., *Numerical modeling in science and engineering*, JohnWiley, New York (1988)
2. Chen, Z., Huan, G., and Ma, Y., *Computational Methods for Multiphase Flows in Porous Media*, SIAM, Dallas, Texas (2006)
3. COMSOL Multiphysics, *User's Guide* Version 3.4, COMSOL AB (2007)
4. Hoteit H., Firoozabadi A., Multicomponent fluid flow by discontinuous Galerkin and mixed methods in unfractured and fractured media, *Water Resources Research*, **41** (2005)
5. Martin, V., Jaffré, J., and Roberts, J., Modeling fractures and barriers as interfaces for flow in porous media, *SIAM*, **26,** 1667–1691 (2005)

10. Acknowledgements

I would like to express my gratitude towards the Mexican Petroleum Institute for supporting me trough a scholarship which allowed me to accomplish my thesis work.